Optical absorption spectra associated with shallow donors in a dielectric quantum well

1996 J. Phys.: Condens. Matter 8 1511

(http://iopscience.iop.org/0953-8984/8/10/021)

J. Phys.: Condens. Matter **8** (1996) 1511–1519. Printed in the UK

Optical absorption spectra associated with shallow donors in a dielectric quantum well

Zhen-Yan Deng†‡

† China Centre of Advanced Science and Technology (World Laboratory), PO Box 8730, Beijing 100080, People's Republic of China
‡ Shanghai Institute of Ceramics, Chinese Academy of Sciences, Shanghai 200050, People's Republic of China

Received 23 August 1995, in final form 10 October 1995

Abstract. We calculate the optical absorption spectra associated with transitions from the $n = 1$ valence subband to the donor level in a dielectric quantum well. It is found that the impurity binding energies evaluated from photoluminescence experiments are lower than the practical binding energies, because of the effect of the image potential on the exciton binding energy in the dielectric quantum well. The broadening of absorption spectra due to the impurity distribution and the fluctuation in well width is also discussed.

1. Introduction

Semiconductor superlattices and heterostructures have been extensively investigated in the last two decades. Progress in this area has been made possible due to the development of sophisticated material growth techniques. The impurity states in these structures have been studied widely in both theoretical and experimental respects [1–10]. A quantum well can be called a dielectric quantum well when the dielectric constant of the barrier material is significantly smaller than that of the well material [11, 12], e.g. the $GaAs/Al_xGa_{1-x}As$ and GaAs/ZnSe quantum well structures. Image charges arise due to the mismatch of dielectric constants at the interfaces. Recently, this topic has received considerable attention [11–22] in studying the electronic, exciton and impurity states in low-dimensional structures. The results showed that the image forces can lead to self-binding of single charges and modify the properties of excitons in quantum wells [12, 13].

In our previous paper [20], we have studied the effect of the image potential on the impurity states in $GaAs/Al_xGa_{1-x}As$ quantum wells. The results indicated that the image potential enhances the impurity binding energy considerably, especially when the width of the quantum well is small. On the other hand, the impurity binding energies in $GaAs/Al_xGa_{1-x}As$ quantum wells obtained from the photoluminescence study [6, 8–10] of impurity states are in good agreement with the binding energies of theoretical prediction which ignore the image potential in quantum wells. Why does this happen? In this paper, we study the problem from a theoretical point of view. In the next section, we outline the theoretical framework. The numerical results and discussion are given in section 3.

0953-8984/96/101511+09$19.50

2. Theory

When the dielectric mismatch between well material and barrier material is considered, in the effective-mass approximation, the Hamiltonians describing the motion of an electron in the dielectric quantum well excluding and including a shallow donor can be written

$$H^{(0)}(\boldsymbol{r}) = V_e(\boldsymbol{r}) + \begin{cases} \dfrac{\boldsymbol{P}^2}{2m_1} & |z| < d_z \\ \dfrac{\boldsymbol{P}^2}{2m_2} + V_0 & \text{elsewhere} \end{cases} \tag{1}$$

and

$$H(\boldsymbol{r}) = H^{(0)}(\boldsymbol{r}) + V_{ion}(\boldsymbol{r}) \tag{2}$$

where $2d_z$ is the width of the quantum well, $\boldsymbol{P}$ and $\boldsymbol{r} = (\rho, \theta, z)$ are the electron momentum and coordinate, respectively, m_1 and m_2 are the electron-band effective mass in the well material and barrier material, respectively, V_0 is the electron-confining potential in the quantum well, which is equal to the conduction- or valence-band discontinuity between the barrier material and well material, $V_e(\boldsymbol{r})$ is the electron image potential and $V_{ion}(\boldsymbol{r})$ is the sum of the impurity ion potential and its image potentials in the dielectric quantum well [20].

The trial wavefunctions for ground electronic and impurity states in the dielectric quantum well can be written [20]

$$\phi_1(\boldsymbol{r}) = N_0 \begin{cases} \exp[k_{2z}(d_z - z)]\cos(k_{1z}d_z) & z \geqslant d_z \\ \cos(k_{1z}z) & |z| \leqslant d_z \\ \exp[k_{2z}(d_z + z)]\cos(k_{1z}d_z) & z \leqslant -d_z \end{cases} \tag{3}$$

and

$$\psi(\boldsymbol{r}) = N\phi_1(\boldsymbol{r})\exp\{-[\rho^2 + (z - z_0)^2]^{1/2}/\lambda\} \tag{4}$$

where N_0 and N are the normalization constants, λ is the variational parameter and $(0, 0, z_0)$ is the position of the donor in the quantum well. The parameters

$$k_{1z} = [2m_1 E_1^{(0)}/\hbar^2]^{1/2} \tag{5a}$$

$$k_{2z} = [2m_2(V_0 - E_1^{(0)})/\hbar^2]^{1/2} \tag{5b}$$

where the ground level $E_1^{(0)}$ without the image potential is determined using the appropriate current-conserving boundary conditions for the wavefunctions at the interfaces and must satisfy the following relation:

$$m_1 k_{2z} = m_2 k_{1z}\tan(k_{1z}d_z). \tag{6}$$

The ground electronic energy level and impurity binding energy in the dielectric quantum well are obtained as follows:

$$E_1 = \langle\phi_1(\boldsymbol{r})|H^{(0)}(\boldsymbol{r})|\phi_1(\boldsymbol{r})\rangle \tag{7}$$

and

$$E_b = E_1 - \min_{\lambda}\langle\psi(\boldsymbol{r})|H(\boldsymbol{r})|\psi(\boldsymbol{r})\rangle. \tag{8}$$

For an optical transition from the first valence subband to a donor level, we have for the initial state

$$|i\rangle = \phi_1(\boldsymbol{r})S^{-1/2}\exp(\mathrm{i}k_\perp\rho\cos\theta)u_i(\boldsymbol{r}) \tag{9}$$

where S is the area of the interface of quantum well and $k_\perp = (k_x^2+k_y^2)^{1/2}$ is the wavevector inside the plane of the quantum well. For the final state, the wavefunction is

$$|f\rangle = \psi(\boldsymbol{r})u_f(\boldsymbol{r}). \tag{10}$$

In equations (9) and (10), $u_i(\boldsymbol{r})$ and $u_f(\boldsymbol{r})$ are the periodic parts of the Bloch state for the initial and final states, respectively.

Taking the energy origin at the bottom of the first conduction subband, we have for the energy of the initial state

$$E_i = -\epsilon_g - \frac{\overline{h}^2}{2m_h}k_\perp^2 \tag{11}$$

where m_h is the effective mass of the valence band in GaAs and

$$\epsilon_g = E_g + E_1^C + E_1^V \tag{12}$$

with E_g being the bulk GaAs band gap and E_1^C (E_1^V) the ground energy level of the first conduction (valence) subband in the quantum well. The energy of the final state is

$$E_f = -E_b(2d_z, z_0) \tag{13}$$

where $E_b(2d_z, z_0)$ is the binding energy of the donor impurity.

The transition probability per unit time for transition from the first valence subband to donor level associated with the impurity located at the position $(0, 0, z_0)$ is proportional to the square of the matrix element of the electron–photon interaction H_{int} between the wavefunctions of the initial state (valence) and final (impurity) state [4, 5]

$$W(\omega, 2d_z, z_0) = \frac{2\pi}{\overline{h}}\sum_i |\langle f|H_{int}|i\rangle|^2\delta(E_f - E_i - \overline{h}\omega) \tag{14}$$

with $H_{int} = C\boldsymbol{e}\cdot\boldsymbol{p}$, where $\boldsymbol{e}$ is the polarization vector in the direction of the electric field of the radiation, $\boldsymbol{p}$ is the momentum operator and C is a pre-factor that describes the effects of the photon vector potential [4, 5]. The above matrix element may be written [4, 5]

$$\langle f|H_{int}|i\rangle \simeq C\boldsymbol{e}\cdot\boldsymbol{P}_{fi}S_{fi} \tag{15}$$

with

$$\boldsymbol{P}_{fi} = \frac{1}{\Omega}\int_\Omega u_f^*(\boldsymbol{r})\boldsymbol{p}u_i(\boldsymbol{r})\,\mathrm{d}\boldsymbol{r} \tag{16}$$

and

$$S_{fi} = \int F_f^*(\boldsymbol{r})F_i(\boldsymbol{r})\,\mathrm{d}\boldsymbol{r} \tag{17}$$

where Ω is the volume of the unit cell and $F_f(\boldsymbol{r})$ ($F_i(\boldsymbol{r})$) is the envelope function for the final (initial) state. Then equation (14) can be simplified further:

$$W(\omega, 2d_z, z_0) = \frac{m_h S}{\overline{h}^3}|C|^2|\boldsymbol{e}\cdot\boldsymbol{P}_{fi}|^2|S_{fi}(z_0, k_\perp(\Delta))|^2 Y(\Delta) \tag{18}$$

where $Y(\Delta)$ is the step function and

$$\Delta = \overline{h}\omega + E_b(2d_z, z_0) - \epsilon_g \tag{19a}$$

$$k_\perp(\Delta) = (2m_h\Delta/\overline{h}^2)^{1/2}. \tag{19b}$$

In the practical doped samples, usually there is a small fluctuation in the well width [9] and the doping of the impurity in the quantum well is not strict δ doping [8]. In this paper, we consider the impurity distribution and the fluctuation in the well width as the Gaussian

functions. The total transition probability per unit time for transition from the first valence subband to the donor level can be obtained:

$$W(\omega) = \int_0^\infty \mathrm{d}(2d_z) \int_{-d_z}^{d_z} \mathrm{d}z_0 \, P_1(z_0) P_2(2d_z) W(\omega, 2d_z, z_0) \tag{20}$$

where

$$P_1(z_0) = P_{10} \exp[-(z_0 - z_0^{(0)})^2/2\alpha] \tag{21a}$$

$$P_2(2d_z) = P_{20} \exp[-(2d_z - 2d_z^{(0)})^2/2\beta] \tag{21b}$$

and the impurity position z_0 and the well width $2d_z$ are in ångströms. The constants P_{10} and P_{20} are determined by the following equations:

$$\int_{-d_z}^{d_z} \mathrm{d}z_0 \, P_1(z_0) = 1 \tag{22b}$$

$$\int_0^\infty \mathrm{d}(2d_z) \, P_2(2d_z) = 1. \tag{22a}$$

The above integrals were calculated numerically.

3. Results and discussion

In our practical calculation, the following parameters are adopted: the electron and hole effective mass and the static dielectric constant are $m_e = 0.067m_0$, $m_h = 0.35m_0$ and $\epsilon_1 = 12.5$ for GaAs, $m_e = 0.15m_0$, $m_h = 0.40m_0$ and $\epsilon_2 = 10.1$ for AlAs, and $m_e = 0.17m_0$, $m_h = 0.76m_0$ and $\epsilon_2 = 7.6$ for ZnSe with m_0 the free-electron mass and the mixing of the light- and heavy-hole bands neglected. The electron-confining potentials for conduction and valence bands are $V_e = 1060$ meV and $V_h = 550$ meV in a GaAs/AlAs quantum well, and $V_e = 340$ meV and $V_h = 960$ meV in a GaAs/ZnSe quantum well [12].

Figure 1 shows the possible optical transitions from the first valence subband to the donor and exciton levels, where $\hbar\omega_1$ and $\hbar\omega_2$ represent the transition energies from the top edge of the first valence subband to the donor and exciton levels, respectively.

Figures 2 and 3 show the optical transition spectra associated with donors in GaAs/AlAs and GaAs/ZnSe quantum wells with different structure parameters, where $E_j = \hbar\omega_j - E_g$ ($j = 1, 2$). In figures 2 and 3, the energy E_2 represents the peak position of the transition from the first valence subband to the exciton level and E_{vc} is the onset of valence-to-conduction-band absorption, and the ground exciton binding energies including and excluding image potential are taken from [12]. In fact, in figure 2 the fluctuation in well width is neglected and only an impurity distribution (half-width of Gaussian distribution, about 5.3 Å) in a quantum well is considered; in figure 3 the impurity distribution is a strict δ distribution and a fluctuation in the well width (half-width of Gaussian distribution, about 4.7 Å) is included. Comparing figure 2 with figure 3, we find that the impurity distribution causes a broadening of the absorption peak on the high-energy side, and the fluctuation in well width leads to broadening of the absorption peak on the low- and high-energy sides simultaneously. Although the impurity distribution and the fluctuation in well width cause broadening of the absorption peak, the peak position of absorption spectra does not apparently change, as shown in figures 2 and 3. From figures 2 and 3, we can also see that the image potential changes the peak positions of absorption spectra considerably, and the effect of the image potential in the GaAs/ZnSe quantum well is larger than that in the GaAs/AlAs quantum well due to the larger dielectric mismatch between GaAs and ZnSe.

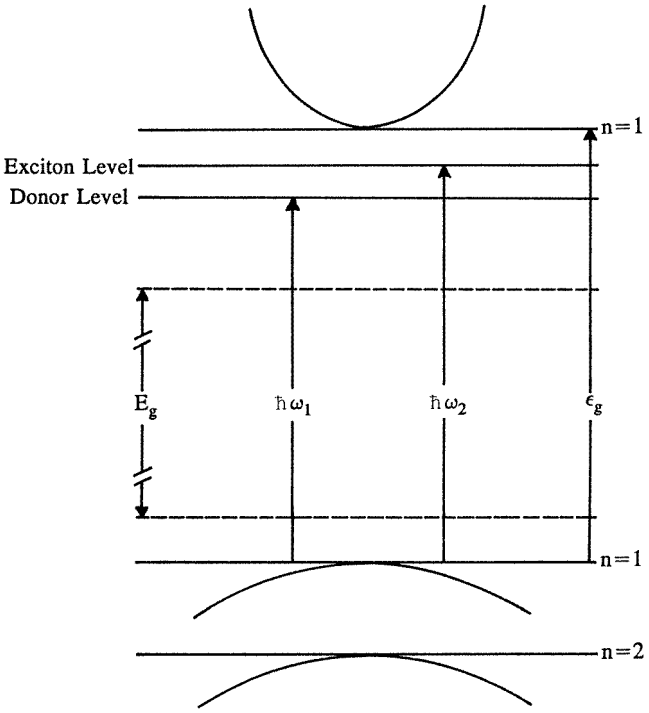

Figure 1. Schematic representation of the possible optical transitions from the first valence subband to the donor and exciton levels in quantum well, where the parabolae represent the energy dispersions of the first conduction and valence subbands inside the plane of quantum well.

In the above discussion, we consider only the absorption spectra for the transition from the first valence subband to the donor level. The photoluminescence lineshape associated with donors in quantum wells is the same as that of absorption spectra [4, 5]. The peaks of photoluminescence spectra that can be observed in the doped quantum wells are exciton peaks and the peak associated with the transition from donor level to the first valence subband [8]. Usually, the donor binding energy evaluated from photoluminescence study is given by the equation [8] $E_b = E_2 - E_1 + E_{e-h}$ where E_1 is the peak position associated with transitions between electrons on donors and the first valence subband states and E_2 is the peak position of the ground heavy-hole exciton. The heavy-hole exciton binding energy E_{e-h} in the above equation is obtained theoretically. In figure 4, we show the difference $E_2 - E_1$ between the peak positions including and excluding the image potential in the GaAs/AlAs and GaAs/ZnSe quantum wells. If we assume that the peak distance $E_2 - E_1$ including the image potential from our theoretical calculation is the practical distance observed from the photoluminescence study, the donor binding energy evaluated from the photoluminescence study in the GaAs/AlAs quantum well is in good agreement with the theoretical binding energy excluding the image potential within the experimental error (± 0.5 meV), as many researchers [6, 8–10] have reported. The difference $E_2 - E_1$ between the peak positions including and excluding the image potential in the GaAs/AlAs quantum well is small (within ± 0.4 meV), as shown in figure 4(a). In fact, these underestimate the donor binding energy $E_b = E_2 - E_1 + E_{e-h}$, because the effect of the image potential on the exciton binding

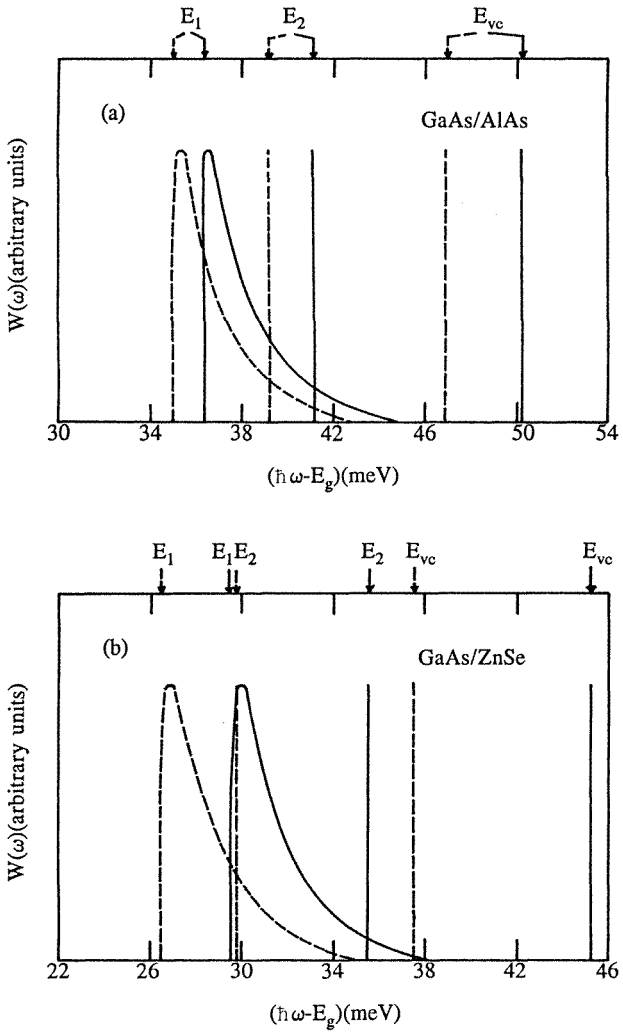

Figure 2. Optical absorption probability per unit time for the transition from the first valence subband to the donor impurity level as a function of $\hbar\omega - E_g$ in (*a*) GaAs/AlAs and (*b*) GaAs/ZnSe quantum wells, where the well width $2d_z^{(0)} = 100$ Å and the impurity is located at the centre of the quantum well, $z_0^{(0)} = 0$, with the parameters $\alpha = 20$ and $\beta \to 0$. The solid and broken curves represent the results including and excluding the image potential, respectively.

energy E_{e-h} is neglected, which is large when the dimension of the quantum well becomes small, as shown in figure 4(*a*). The situation in the GaAs/ZnSe quantum well is different from that in the GaAs/AlAs quantum well, because the difference $E_2 - E_1$ between the peak positions including and excluding the image potential in the GaAs/ZnSe quantum well is large, as shown in figure 4(*b*), due to a larger dielectric mismatch between GaAs and ZnSe. It is expected that the donor binding energy evaluated from the photoluminescence study in the doped GaAs/ZnSe quantum well is larger than the theoretical binding energy excluding the image potential. If the effect of the image potential on the exciton binding energy is

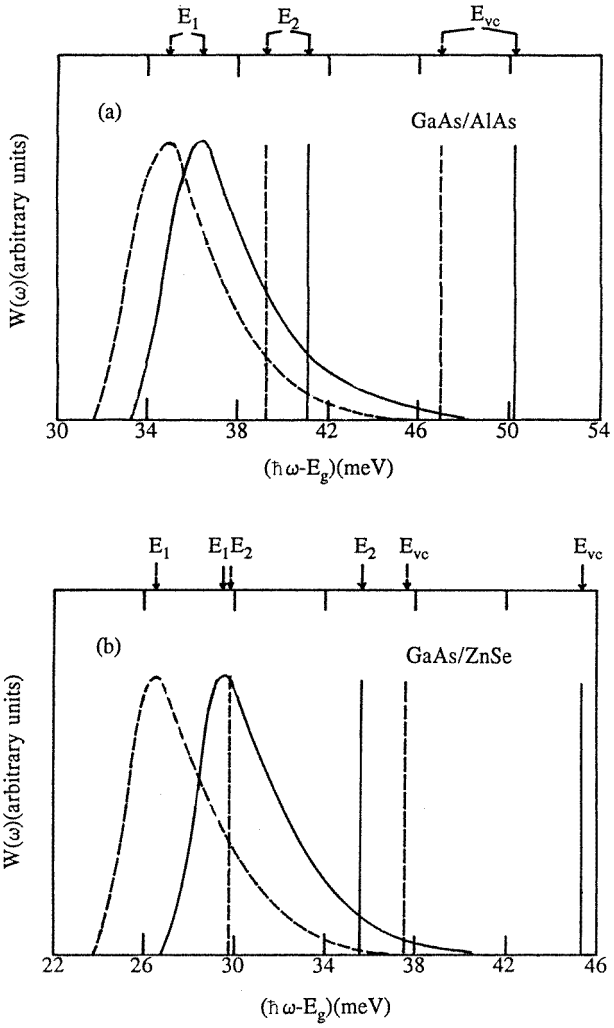

Figure 3. Optical absorption probability per unit time for the transition from the first valence subband to the donor impurity level as a function of $\overline{\hbar}\omega - E_g$ in (*a*) GaAs/AlAs and (*b*) GaAs/ZnSe quantum wells, where the well width $2d_z^{(0)} = 100$ Å and the impurity is located at the centre of the quantum well, $z_0^{(0)} = 0$, with the parameters $\alpha \to 0$ and $\beta = 16$. The solid and broken curves represent the results including and excluding the image potential, respectively.

considered, the impurity binding energy evaluated from the photoluminescence experiment should be in good agreement with the theoretical binding energy which includes the image potential [20].

In conclusion, we have studied the optical absorption spectra associated with transition from the $n = 1$ valence subband to the donor level in the dielectric quantum wells. Our results indicate that the donor binding energy evaluated from the photoluminescence study is lower than the practical binding energy, if the effect of the image potential on the exciton binding energy is neglected. The results also indicate that the impurity distribution causes a broadening of absorption peak on the high-energy side, and the fluctuation in well width

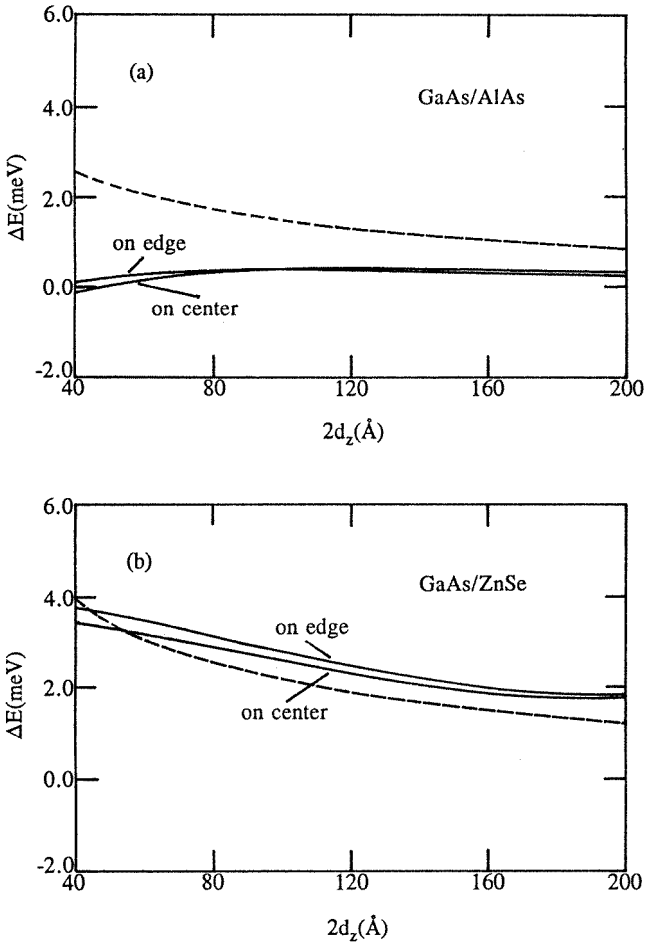

Figure 4. Variations in the difference $E_2 - E_1$ between the peak positions including and excluding the image potential with the well width (solid curves) in (*a*) GaAs/AlAs and (*b*) GaAs/ZnSe quantum wells for an impurity at the edge and the centre in the quantum well. The broken curves represent the difference between the heavy-hole exciton binding energy including and excluding the image potential, which are taken from [12].

leads to broadening of the absorption peak on the low- and high-energy sides simultaneously. However, the impurity distribution and the fluctuation in well width do not change the peak position of the absorption spectra. Hopefully the theoretical results will stimulate further experiment investigation.

References

[1] Bastard G 1981 *Phys. Rev.* B **24** 4714
[2] Mailhiot C, Chang Y C and McGill T C 1982 *Phys. Rev.* B **26** 4449
[3] Stopa M and DasSarma S 1989 *Phys. Rev.* B **40** 8466
[4] Oliveira L E and Perez-Alvarez R 1989 *Phys. Rev.* B **40** 10 460
[5] Santiago R B, Castro J A and Oliveira L E 1993 *Phys. Rev.* B **48** 4498
[6] Miller R C, Gossard A C, Tsang W T and Munteanu O 1982 *Phys. Rev.* B **25** 3871

[7] Shanabrook B V, Comas J, Perry T A and Merlin R 1984 *Phys. Rev.* B **29** 7096
[8] Liu X, Petrou A, McCombe B D, Ralston J and Wicks G 1988 *Phys. Rev.* B **38** 8522
[9] Rune G C, Holtz P O, Sundaram M, Merz J L, Gossard A C and Monemar B 1991 *Phys. Rev.* B **44** 4010
[10] Adelabu J S A 1985 *Physica* B **205** 65
[11] Cen J and Bajaj K K 1993 *Phys. Rev.* B **48** 8061
[12] Cen J, Chen R and Bajaj K K 1994 *Phys. Rev.* B **50** 10 947 and references therein
[13] Babiker M 1993 *J. Phys.: Condens. Matter* **5** 2137, and references therein
[14] Cappellini G and Delsole R 1991 *Solid State Commun.* **79** 185
[15] Elabsy A M 1992 *Phys. Rev.* B **46** 2621
[16] Dostov V L and Wang Z G 1994 *Semicond. Sci. Technol.* **9** 1781
[17] Zhao Q X, Pasquarello A, Holtz P O, Monemar B and Willander M 1994 *Phys. Rev.* B **50** 10 953
[18] Deng Z Y and Gu S W 1993 *J. Phys.: Condens. Matter* **5** 2261
[19] Deng Z Y, Guo J K and Lai T R 1994 *J. Phys.: Condens. Matter* **6** 5949
[20] Deng Z Y, Lai T R and Guo J K 1994 *Phys. Rev.* B **50** 5732
[21] Li Z W and Gao S W 1994 *Phys. Rev.* B **50** 15 349
[22] Fischer R and Fauster T 1995 *Phys. Rev.* B **51** 7112